frontiers | Frontiers in Chemistry

TYPE Original Research
PUBLISHED 04 January 2023
DOI 10.3389/fchem.2022.1104844

Check for updates

OPEN ACCESS

EDITED BY
Xifei Li,
Xi'an University of Technology, China

REVIEWED BY
Di Wu,
Washington State University,
United States
Dan Li,
Sichuan University, China

*CORRESPONDENCE
Sai Zhang,
zhangsai1112@nwpu.edu.cn
Yuanyuan Ma,
yyma@nwpu.edu.cn

SPECIALTY SECTION
This article was submitted to
Electrochemistry,
a section of the journal
Frontiers in Chemistry

RECEIVED 22 November 2022
ACCEPTED 14 December 2022
PUBLISHED 04 January 2023

CITATION
Zhang M, Zhang S and Ma Y (2023), *In-situ* reconstruction of $CoBO_x$ enables formation of Co for synthesis of benzylamine through reductive amination.
Front. Chem. 10:1104844.
doi: 10.3389/fchem.2022.1104844

In-situ reconstruction of $CoBO_x$ enables formation of Co for synthesis of benzylamine through reductive amination

Mingkai Zhang[1,2], Sai Zhang[1]* and Yuanyuan Ma[1]*

[1]Key Laboratory of Special Functional and Smart Polymer Materials of Ministry of Industry and Information Technology, School of Chemistry and Chemical Engineering, Northwestern Polytechnical University, Xi'an, China, [2]Frontier Institute of Science and Technology, Xi'an Jiaotong University, Xi'an, China

Cobalt (Co) as a substitute of noble-metal catalysts shows high catalytic capability for production of the widely used primary amines through the reductive amination. However, the synthesis of Co catalysts usually involves the introduction of organic compounds and the high-temperature pyrolysis, which is complicated and difficult for large-scale applications. Herein, we demonstrated a facile and efficient strategy for the preparation of Co catalysts through the *in situ* reconstruction of cobalt borate ($CoBO_x$) during the reductive amination, delivering a high catalytic activity for production of benzylamine from benzaldehyde and ammonia. Initially, $CoBO_x$ was transformed into $Co(OH)_2$ through the interaction with ammonia and subsequently reduced to Co nanoparticles by H_2 under the reaction environments. The *in situ* generated Co catalysts exhibited a satisfactory activity and selectivity to the target product, which overmatched the commonly used Co/C, Pt or Raney Ni catalysts. We anticipate that such an *in situ* reconstruction of $CoBO_x$ by reactants during the reaction could provide a new approach for the design and optimization of catalysts to produce primary amines.

KEYWORDS

heterogeneous catalysis, reductive amination, primary amine, in-situ reconstruction, cobalt

1 Introduction

Primary amines are essential raw materials and intermediates in fine chemical industry, playing significant roles in the synthesis of pharmaceuticals, biomolecules, advanced polymers, and agrochemicals (Kim et al., 2013; Cabrero-Antonino et al., 2019; Afanasyev et al., 2020; Irrgang and Kempe, 2020; Murugesan, et al., 2020). Various strategies have been investigated to synthesize primary amines, including reductive amination (Ball et al., 2018; Murugesan et al., 2019; Sukhorukov, 2020), aryl halides amination (Schranck and Tlili, 2018; Wang et al., 2022), nitriles hydrogenation (Garduño and García, 2020; Lévay and Hegedűs, 2018; Chen et al., 2016), olefins hydroamination

TABLE 1 Comparison on different Co-based catalysts in reductive amination.

Number	Catalyst	Reaction conditions	Yield of benzylamine (%)	Ref
1	Co@NC-700	110°C, $NH_3{\cdot}H_2O$, 2 MPa H_2	92	Liu et al., 2019
2	Co@NC-ligand-800	120°C, 0.5–0.7 MPa NH_3	74	Ma et al., 2022
3	Co-DABCO-TPA@C-800	120°C, 0.5–0.7 MPa NH_3, 4 MPa H_2	87	Jagadeesh et al. (2017)
4	Co@NC-800	130°C, $NH_3{\cdot}H_2O$, 1 MPa H_2	97	Yuan et al., 2019
5	Co-salen complexes	120°C, 0.5 MPa NH_3, 4.5 MPa H_2	89	Senthamarai et al. (2020)

(Miller et al., 2019; Sengupta et al., 2020), etc. Owing to the application of economical ammonia as well as the accessible reaction engineering, the reductive amination with usage of ammonia as the nitrogen resource represents one of the most cost-effective methods to manufacture primary amines. However, this process usually suffers from the selectivity challenge due to the side reactions including over hydrogenation of imines and reduction of carbonyl compounds to the corresponding alcohols (Chandra et al., 2018; Gallardo-Donaire et al., 2018). Thus, to design the appropriate catalyst to achieve selective production of primary amines through the reductive amination is highly desired.

Both traditional homogeneous metal complexes and heterogeneous catalysts have been successfully applied to produce primary amines through reductive amination, in which heterogeneous catalysts are more applicable in industrial field with the advantages of good durability, easy recycling and high potential for scale-up. Previously, noble metal-based catalysts (Pt, Pd, Ru, Rh, etc.) have exhibited satisfactory selectivity for target product (Dong et al., 2015; Nakamura et al., 2015; Chatterjee et al., 2016; Komanoya et al., 2017; Liang et al., 2017; Guo et al., 2019; Dong et al., 2020; Jv et al., 2020; Qi et al., 2021). Nevertheless, the high price of noble metals increases the production cost and limits the practical application. Consequently, the development of the non-noble metal-based heterogeneous catalysts is highly expected.

On account of the relatively high abundance and low price, Co has been employed as a reasonable non-noble metal-based catalysts in reductive amination among different substitutes for noble metals. As shown in Table 1, several heterogeneous Co-based catalysts were successfully reported (Jagadeesh et al., 2017; Liu et al., 2019; Yuan et al., 2019; Senthamarai et al., 2020; Ma et al., 2022), including Co-DABCO-TPA@C-800, Co@NC-800, Co/mCN-900, etc. With Co nanoparticles as the active sites, these catalysts delivered satisfactory reactivity and realized the selective synthesis of benzylamine. Generally, the synthesis of the reported Co nanocatalysts was achieved through the thermal pyrolysis of various organometallic cobalt complexes. Although such synthetic method has been proved efficacious to prepare Co-based catalysts, the complicated operating procedures and high-temperature pyrolysis constrain its further application. Thus, an alternative method with the simplified procedure and mild condition is highly demanded.

Herein, we reported a facile method to prepare Co catalysts through the *in situ* reconstruction of $CoBO_x$ under the reductive amination environment, which delivered a high catalytic activity for the production of benzylamine between benzaldehyde and ammonia. In this method, the original $CoBO_x$ reacted with ammonia to yield surface $Co(OH)_2$ initially, which was then reduced by hydrogen (H_2) to form Co nanoparticles during the reductive amination. In comparison with the previously reported strategies to prepare Co catalysts, such reconstructed Co catalysts realized the *in situ* formation of Co active sites and avoided the introduction of organic complexes as well as the high-temperature pyrolysis, in accordance with the requirements for green chemistry. The *in situ* synthesized Co catalysts delivered high capability for the selective conversion of benzaldehyde and ammonia towards benzylamine (> 95%). This reconstruction synthetic method may provide a new approach for the design of non-noble metal-based heterogeneous catalysts for reductive amination.

2 Materials and methods

2.1 Synthesis of catalysts

2.1.1 Synthesis of $CoBO_x$

Based on a previous work (Chen et al., 2016), the $CoBO_x$ nanosheets were synthesized through a facile and scalable wet chemistry method. Typically, 3 mmol of $Co(NO_3)_2{\cdot}6H_2O$ and 7.5 mmol of $NaBH_4$ were dissolved in 285 ml and 15 ml distilled water, respectively. Then, the freshly prepared aqueous $NaBH_4$ solution was added into the $Co(NO_3)_2$ solution and the mixture was placed under the stirring of 800 rpm at room temperature for 1 h. After 2 h of aging, the solids were centrifuged off and washed by distilled water and ethanol alternatively for three times. Finally, the collected $CoBO_x$ was dried at 60°C for 12 h in a vacuum oven and then stored for future use.

2.1.2 Synthesis of C and SiO_2 supports

C supports were synthesized from the nitric acid treatment of the commercial carbon black. The details could be found in a previous report (Zhang et al., 2022). To synthesize SiO_2 supports, 300 mg of the commercial SiO_2 was well dispersed in 50 ml of ethanol, then 100 µl of 3-(Trimethoxysilyl)-1-propanamine was added into the suspension. Next, the mixture was heated under 90°C for 4 h and washed by ethanol for three times. Finally, the prepared SiO_2 was dried at 60°C for 24 h and stored in a vacuum oven.

2.1.3 Synthesis of Pt-based catalysts

The Pt/C catalysts were synthesized through an impregnation method. Firstly, 300 mg of the nitric acid-treated carbon black was well dispersed in 30 ml of distilled water by ultrasonication. Then, 0.75 ml of 2 mg ml^{-1} of $Na_2PtCl_6·6H_2O$ was added and the suspension was placed under the stirring of 800 rpm for 1 h at room temperature. Afterwards, the mixture was heated at 80°C until the complete evaporation of the solution and the collected solid was treated under H_2/Ar atmosphere at 300°C for 2 h. Finally, the Pt/C catalysts were dried in vacuum at 60°C for 12 h. The Pt/SiO_2 catalysts were prepared through the similar procedure.

2.1.4 Synthesis of Co/C

To synthesize Co/C catalysts, 300 mg of the nitric acid-treated carbon black was well dispersed in 30 ml of distilled water by ultrasonication. Then, 3 ml of 5 mg ml^{-1} $Co(NO_3)_2·6H_2O$ solution was added and the suspension was placed under the stirring of 800 rpm for 1 h at room temperature. Afterwards, the mixture was heated at 80°C until the complete evaporation of the solution and the collected solid was treated under H_2/Ar atmosphere at 300°C for 2 h with a heating rate of 5°C/min. Finally, the Co/C catalysts were dried and stored in a vacuum oven.

2.1.5 Synthesis of $Co(OH)_2$ and Co_3O_4

To synthesize $Co(OH)_2$, 1.16 g of $Co(NO_3)_2·6H_2O$ and 19.2 g of NaOH were dissolved in 10 ml and 70 ml of distilled water, respectively. After 1 h of rigorous stirring, the two solutions were mixed and then transferred to a 100 ml of stainless autoclave. After 100°C of hydrothermal for 24 h, the solids were centrifuged off and washed by distilled water and ethanol alternatively for three times. Finally, the collected $Co(OH)_2$ was dried at 60°C in a vacuum oven for 12 h and then stored for future use. For the synthesis of Co_3O_4, 300 mg of the as-synthesized $CoBO_x$ was calcinated at 500°C under air for 3 h, then the solids were collected and stored after cooling to room temperature.

2.2 Characterizations

Transmission electron microscopy (TEM) measurements were conducted on Hitachi HT-7700 with the accelerating voltage of 120 kV. High resolution transmission electron microscopy (HRTEM) was performed on a JEOL JEM-F200 microscope with an accelerating voltage of 200 kV. X-ray diffraction (XRD) patterns were acquired from a Rigaku Powder X-ray diffractometer with the Cu Kα radiation, and X-ray photoelectron spectra (XPS) were obtained on a Thermo Electron Model K-Alpha with Al Kα as the excitation sources.

2.3 Catalytic reaction

The reductive amination of benzaldehyde and aqueous ammonia was carried out in a 30 ml of stainless autoclave. Initially, the $CoBO_x$ catalysts, benzaldehyde, ammonia and isopropanol with the desired amounts were mixed in the autoclave. Next, the stainless autoclave was pressurized with 2 MPa of H_2, and the reaction temperature was raised to 80°C with a heating rate of 5°C/min. Finally, the reaction was processed under the stirring (600 rpm) at 80°C. When the reaction finished, the reaction mixture was centrifugated off and diluted with ethyl acetate. After the dehydration by anhydrous magnesium sulfate, the reaction products were analyzed by gas chromatography. The conversion of benzaldehyde (X) and the product selectivity (S_i) were calculated by the following equations:

$$X\,(\%) = \frac{[Benzaldehyde]_0 - [Benzaldehyde]_t}{[Benzaldehyde]_0} \times 100$$

$$S_i\,(\%) = \frac{[Product]_i \times N_i}{[Benzaldehyde]_0 - [Benzaldehyde]_t} \times 100$$

Where $[Benzaldehyde]_0$ and $[Benzaldehyde]_t$ were the initial concentration and the residual concentration of benzaldehyde, respectively. $[Product]_i$ was the concentration of the product i in the residual mixture and N_i was the stoichiometric coefficient for product i with reference to benzaldehyde.

3 Results and discussion

The morphology of the as-synthesized $CoBO_x$ catalysts was examined by the transmission electron microscopy. As shown in Figures 1A, B, the as-synthesized $CoBO_x$ nanomaterials exhibited a nanosheet morphology with the smooth surface. No XRD characteristic peaks were observed for the $CoBO_x$ nanosheets, indicating their amorphous feature (Figure 1C). Afterwards, the valence state of Co element in $CoBO_x$ catalysts was analyzed by XPS. As shown in Figure 1D, Co^{2+} primarily existed on the surface of $CoBO_x$, indicated by the characteristic peaks at 780.9 eV and the presence of a satellite peak. Meanwhile, there was no apparent peak at approximate 778.0 eV, further confirming the absence of Co^0 in the as-synthesized nanosheets.

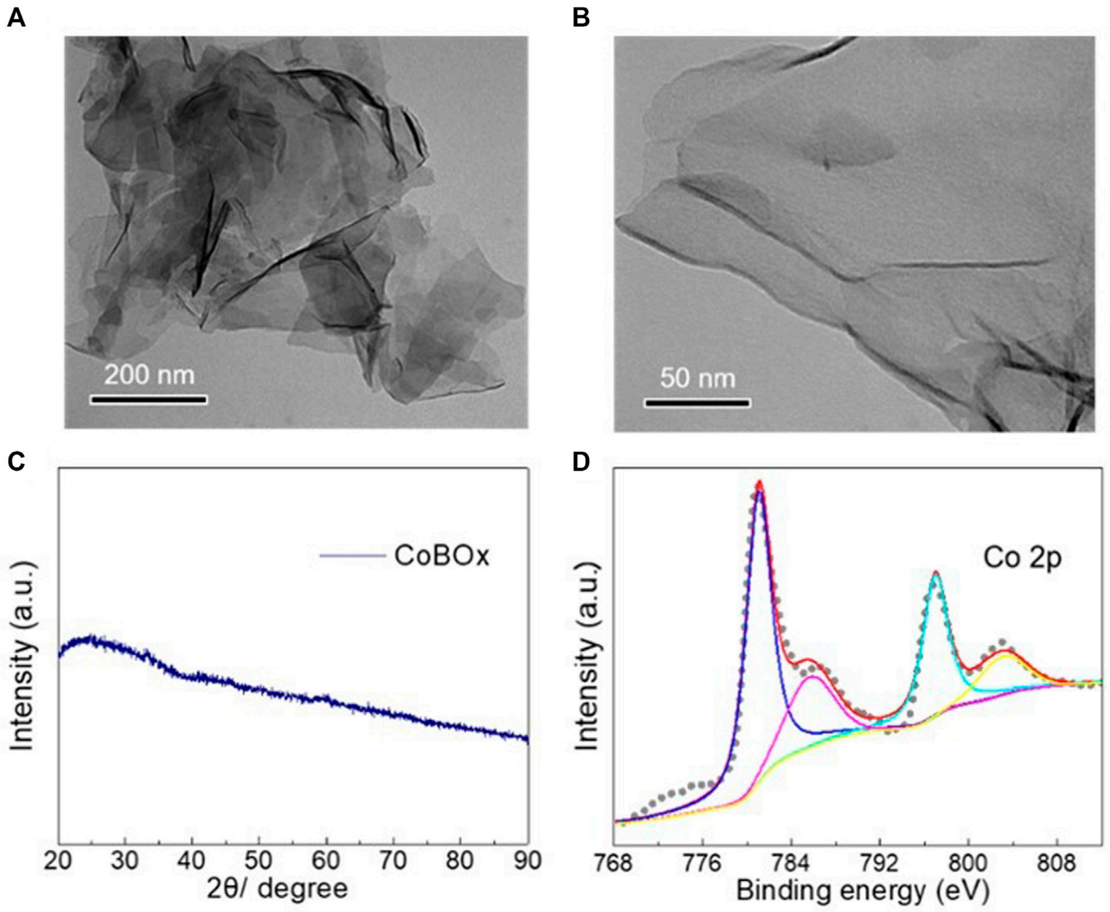

FIGURE 1
Characterizations of the fresh $CoBO_x$ catalysts. **(A,B)** TEM images of the $CoBO_x$ nanosheets with different magnification times. **(C)** XRD pattern and **(D)** XPS spectrum of Co 2p of the $CoBO_x$ nanosheets.

The reductive amination between benzaldehyde and aqueous ammonia (25 *wt*%–28 *wt*%) to produce benzylamine was applied to explore the *in situ* reconstruction of $CoBO_x$ as well as the catalytic performance. Generally, the following steps are included in the reductive amination of benzaldehyde and ammonia into benzylamine (Figure 2A): (I) the condensation between benzaldehyde and ammonia to generate benzylideneimine; (II) the reduction of benzylideneimine to benzylamine; (III) the condensation between the produced benzylamine and benzaldehyde to intermediate *N*-benzylidenebenzylamine; and (IV) the following reductive amination of *N*-benzylidenebenzylamine to target product benzylamine (product 1). Nevertheless, the side reactions of (V) the hydrogenation of benzaldehyde into benzyl alcohol (product 2) and (VI) the over-hydrogenation of *N*-benzylidenebenzylamine (product 3) into dibenzylamine (product 4) decrease the selectivity of the target product, limiting the practical application of this process.

Considering the cation exchange between Co^{2+} and NH_4^+ ions of ammonia and the existence of hydrogen in this reaction system, Co nanoparticles could be reconstructed on the surface of $CoBO_x$ in the presence of ammonia with a high concentration and H_2. To further examine this possibility, the $CoBO_x$ nanosheets were mixed with ammonia, benzaldehyde, and isopropanol (IPA) under 80°C and 2 MPa of H_2 for 15 h. Afterwards, the treated $CoBO_x$ was centrifuged off and characterized in comparison with the freshly prepared $CoBO_x$. Different from the as-synthesized $CoBO_x$ with the light grey color and fluffy accumulation, the treated $CoBO_x$ was in black color with a needle-like appearance, which displayed a strong magnetic response (Supplementary Figure S1). Considering the strong magnetism of the metallic Co, the as-synthesized $CoBO_x$ might be *in situ* transformed into Co nanoparticles in the presence of ammonia and H_2.

Afterwards, the treated $CoBO_x$ was analyzed by various characterizations. Derived from the dark field TEM and

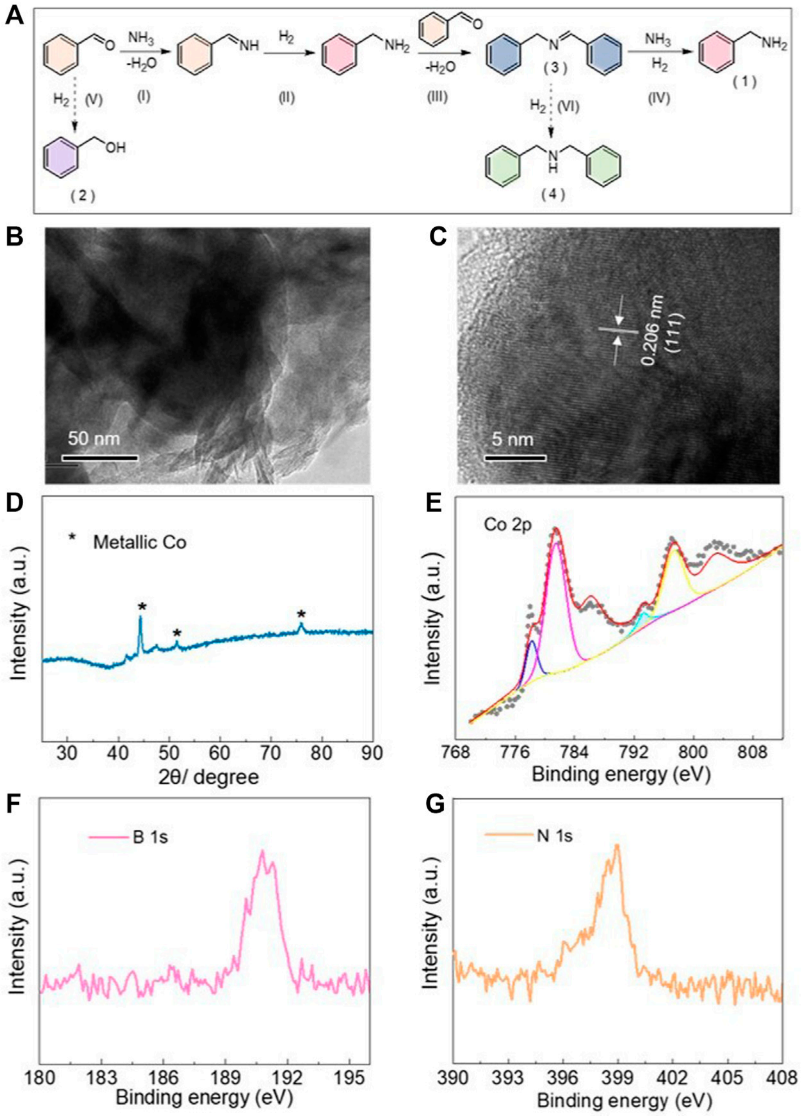

FIGURE 2
(A) Possible reaction pathway for the reductive amination between benzaldehyde and ammonia. **(B)** TEM and **(C)** HRTEM images of the reconstructed $CoBO_x$. **(D)** XRD pattern and **(E)** XPS spectrum of Co 2p of the treated $CoBO_x$. **(F)** XPS spectrum of B 1s and **(G)** N 1s of the treated $CoBO_x$.

HRTEM (Figures 2B, C), the morphology of the treated $CoBO_x$ was totally distinguished from the as-synthesized $CoBO_x$. The original nanosheet structure was obviously destructed. As shown in Figure 2C, the measured lattice fringe spacing of 0.206 nm was observed, which was consistent with that of Co (111) crystal plane, suggesting the existence of Co nanoparticles in the treated $CoBO_x$. In addition, the formation of the Co nanoparticles was further revealed from its XRD pattern. As shown in Figure 2D, the XRD pattern of the treated $CoBO_x$ was in accordance with that of metallic Co (PDF 15–0806), in which a sharp peak could be found around 44.5°, and other small peaks was approximate in 51.6° and 76.1°, respectively. Besides, small peaks at around 41.7° and 47.8° could be attributed to the formation of Co_2B. To further prove the existence of the Co^0, XPS measurements were also employed. As shown in XPS spectrum of Co 2p (Figure 2E), the characteristic peak at 778.1 eV and the peak at 780.9 eV as well as satellite peak indicated the co-existence of Co^0 and Co^{2+} in the reconstructed catalysts. The derived fraction of Co^0 was only 14.7%, which could be attributed to the residual $CoBO_x$ as well as the oxidation of cobalt upon the exposure of catalysts in air during the measurements. In addition, apparent peaks observed on B 1s and N 1s spectrum revealed the presence of B and N

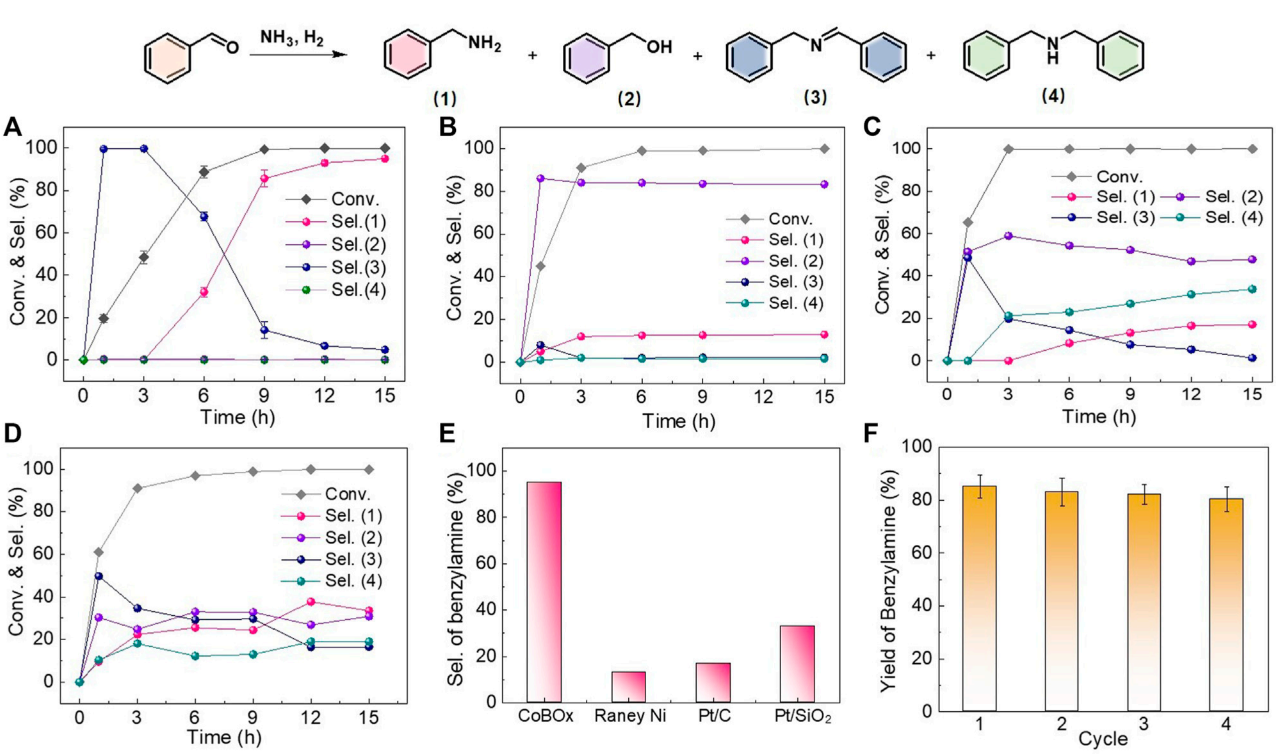

FIGURE 3

Catalytic performance of **(A)** CoBO$_x$, **(B)** Raney Ni, **(C)** Pt/C and **(D)** Pt/SiO$_2$ catalysts. **(E)** Comparison on the selectivity of benzylamine at the end of the reaction. **(F)** Cycling test of CoBO$_x$ catalysts. Reaction conditions: 0.5 mmol benzaldehyde, 80°C, 2 MPa H$_2$, 4 ml IPA, 20 mg CoBO$_x$, or 20 mg 0.5 *wt%* Pt/C, 20 mg 0.5 *wt%* Pt/SiO$_2$, or 5 mg Raney Ni catalysts. The error bars in **(A,F)** were calculated based on three trials.

along with the generation of Co nanoparticles (Figures 2F, G). The XPS results were in accordance with that of TEM and XRD tests, suggesting the successful *in situ* generation of Co nanoparticles. As expected, the original CoBO$_x$ nanosheets could react with ammonia under H$_2$ atmosphere during the reductive amination of benzaldehyde and ammonia.

Then, the catalytic performance of the reconstructed Co nanoparticles was performed for the reductive amination between benzaldehyde and ammonia. After the optimization of solvent (Supplementary Figure S2), the reaction was conducted in isopropanol under 2 MPa of H$_2$ and 80°C. Meanwhile, the catalytic performance of the Raney Ni, Pt/C, and Pt/SiO$_2$ as the controlled catalysts was also examined. When the reconstructed CoBO$_x$ was used as the catalysts (Figure 3A), benzaldehyde was converted to intermediate *N*-benzylidenebenzylamine at the initial 3 h (Step I-III), and further hydrogenated to the target benzylamine as reaction proceeded (Step IV). Finally, the conversion of benzaldehyde reached to > 99% with a selectivity of benzylamine of 95.2% at 15 h. Except for the intermediate *N*-benzylidenebenzylamine and the target product benzylamine, by products of benzyl alcohol and dibenzylamine were not detected, indicating the high reactivity and chemoselectivity of the reconstructed CoBO$_x$ catalysts. In contrast, the main product appeared to be benzyl alcohol on Raney Ni. The selectivity of benzylamine was only 12.1% after the 15 h, indicating that the Step V was predominant on Raney Ni (Figure 3B). On Pt-based catalysts, by products of benzyl alcohol and dibenzylamine were both detected, indicating the occurrence of the Step V and Step VI. The selectivity of benzylamine on Pt/C and Pt/SiO$_2$ were 17.1% and 33.6%, respectively (Figures 3C, D). According to the experimental results, the Co nanoparticles generated from the *in situ* reconstruction of CoBO$_x$ could effectively inhibit the side reactions of benzaldehyde direct hydrogenation and *N*-benzylidenebenzylamine over hydrogenation, avoiding the production of by-products and exhibiting a superior selectivity towards benzylamine in the reductive amination between benzaldehyde and ammonia. As shown in Figure 3E, the selectivity of benzylamine on CoBO$_x$ was 7.9, 5.6, and 2.8 times of that on Raney Ni, Pt/C and Pt/SiO$_2$, respectively.

Afterwards, the stability of the *in situ* formed Co nanoparticles was examined by cycling test. Due to the strong magnetism, the used catalysts could be easily separated from the reaction mixture by a magnet. Without other treatments, the collected catalysts were applied for the next cycle on the identical reaction conditions. As shown in Figure 3F, the reaction time was

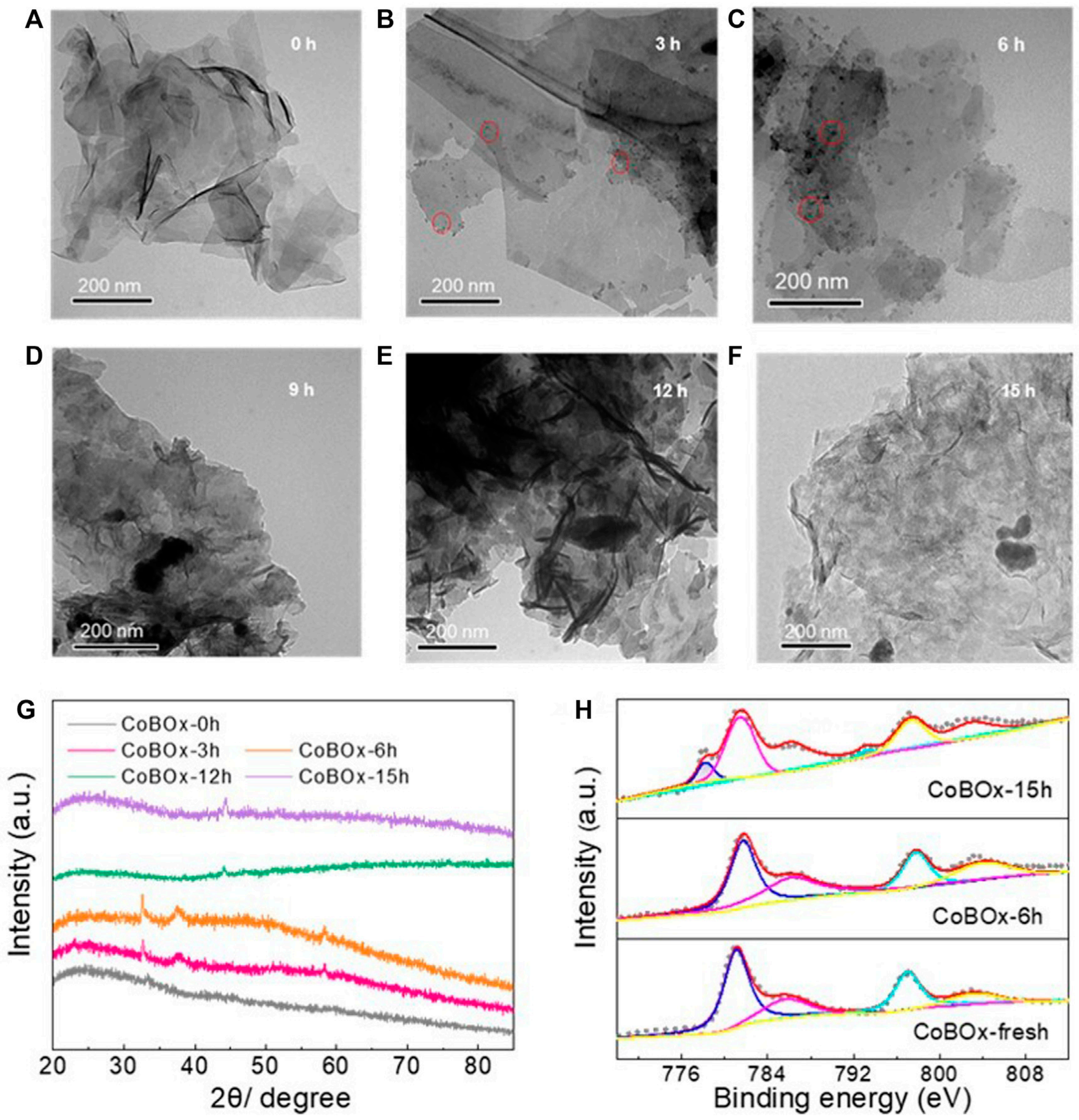

FIGURE 4
TEM images of **(A)** $CoBO_x$-fresh, **(B)** $CoBO_x$-3 h, **(C)** $CoBO_x$-6 h, **(D)** $CoBO_x$-9 h, **(E)** $CoBO_x$-12 h, **(F)** $CoBO_x$-15 h **(G)** XRD pattern and **(H)** XPS spectrum of Co 2p of different $CoBO_x$ catalysts.

controlled as 9 h and the catalysts could be reused at least four cycles with the yields of benzylamine maintained over 80%, suggesting the good catalytic stability of the *in situ* formed Co nanoparticles. Meanwhile, the reaction mixture was analyzed by inductively coupled plasma optical emission spectrometer (ICP-OES), and Co was not detected. The slight reduction of the yield of benzylamine might be resulted from the catalyst loss during the cycling test.

Based on the characterizations and the experimental results, it could be confirmed that $CoBO_x$ could react with ammonia and H_2 under the reductive amination environments, resulting in the formation of Co nanoparticles through the *in situ* reconstruction. Moreover, the Co nanoparticles efficiently suppressed the side reactions and realized the selective production of benzylamine. In order to clarify the active sites on the reconstructed $CoBO_x$, various Co-based catalysts were prepared. As shown in Supplementary Table S1, Co_3O_4 and $Co(OH)_2$ were synthesized by the calcination of $CoBO_x$ and the hydrothermal of $Co(NO_3)_2 \cdot 6H_2O$, respectively (Supplementary Figures S3, S4). The yield of benzylamine was below 1% when catalyzed by either Co_3O_4 or $Co(OH)_2$. Thus, the metallic Co should play a significant role in the production of benzylamine.

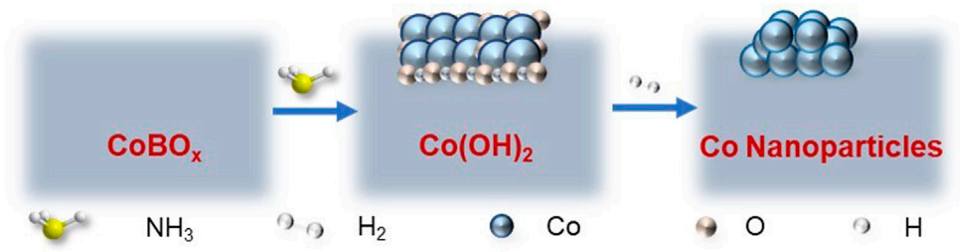

SCHEME 1
Formation of Co through *in situ* reconstruction of $CoBO_x$.

Afterwards, the Co/C catalysts were prepared and employed in this reaction, presenting an obvious lower yield of benzylamine (40.0%) compared with the *in situ* generated Co nanoparticles. As a result, the high selectivity of re-constructed $CoBO_x$ was not only attributed to the formation of metallic Co, but also the *in situ* catalytic environment.

Afterwards, the reconstruction pathway of $CoBO_x$ was explored. The reconstruction of $CoBO_x$ should be a dynamic process, including the reduction of Co^{2+} to Co^0 and the crystallization of metallic Co. To further investigate the dynamic change of $CoBO_x$ during the reductive amination between benzaldehyde and ammonia, the catalysts were collected after the 3 h, 6 h, 9 h, 12 h, and 15 h reaction, respectively, which are named by $CoBO_x$-3 h, $CoBO_x$-6 h, $CoBO_x$-9 h, $CoBO_x$-12 h, $CoBO_x$-15 h. After the thoroughly washing and vacuum drying, these catalysts were analyzed. According to TEM images, it could be observed that nanoparticles were formed on the surface of $CoBO_x$ during the reaction and they aggregated and grew up as reaction proceeded (Figures 4B, C). To further demonstrate the reconstruction of $CoBO_x$, XRD and XPS tests were performed on the various $CoBO_x$ catalysts. According to Figure 4G, the peaks at 32.6°, 38.1°, and 58.2° were observed on $CoBO_x$-3 h and $CoBO_x$-6 h, which was in consistent with the characteristic peaks of $Co(OH)_2$ (PDF no. 51–1731), indicating the formation of $Co(OH)_2$ from $CoBO_x$ during the first 6 h of the reaction. As the reaction continued, the characteristic peaks of $Co(OH)_2$ disappeared, and the typical peaks of metallic Co were observed, indicating the reduction of $Co(OH)_2$ to Co nanoparticles. Moreover, the XPS analysis exhibited the similar phenomenon, in which Co^0 peaks couldn't be found on the original $CoBO_x$ and $CoBO_x$-6 h, but existed in $CoBO_x$-15 h (Figure 4H).

Integrating the results of TEM, XRD, and XPS, the *in situ* reconstruction of $CoBO_x$ might be summarized into the following steps: 1) Given the high concentration of ammonia (~4.5 mmol/ml) in the reaction system, NH_4^+ and OH^- could be easily formed through ionization and separately reacted with $CoBO_x$ (Eq. 1). Consequently, Co^{2+} in $CoBO_x$ could be substituted by NH_4^+ and then interacted with OH^-, resulting in the formation of $Co(OH)_2$ (Eqs 2, 3). 2) Under H_2 atmosphere, $Co(OH)_2$ was finally reduced to Co nanoparticles (Eq. 4). The chemical formulas of $CoBO_x$ reconstruction process are shown below:

$$NH_3 + H_2O \leftrightarrow NH_4^+ + OH^- \quad (1)$$

$$CoBO_x + NH_4^+ \rightarrow (NH_4)_2BO_x + Co^{2+} \quad (2)$$

$$Co^{2+} + OH^- \rightarrow Co(OH)_2 \quad (3)$$

$$Co(OH)_2 + H_2 \rightarrow Co + H_2O \quad (4)$$

As discussed above, the *in situ* reconstruction of $CoBO_x$ follows the order of $CoBO_x \rightarrow Co(OH)_2 \rightarrow$ Co nanoparticles, with which benzaldehyde is selectively transformed to the target product benzylamine. The whole reconstruction process is demonstrated in Scheme 1. According to Scheme 1, ammonia and H_2 play significant roles in the *in situ* reconstruction of $CoBO_x$. To further investigate the influences of ammonia volume and H_2 pressure, the $CoBO_x$ nanosheets were treated under different volume of ammonia and pressure of H_2. As shown in Supplementary Table S2, only when the volume of ammonia > 2 ml and the pressure of H_2 > 2 MPa could the $CoBO_x$ be *in situ* reconstructed. Thus, adequate ammonia volume and H_2 pressure are necessary for the *in situ* reconstruction of $CoBO_x$. Besides, NaOH was also applied to replace ammonia, it turned out that Co nanoparticles were not formed, further confirming the indispensability of ammonia.

4 Conclusion

In this work, we reported the formation of Co nanoparticles through the *in situ* reconstruction of $CoBO_x$ during the reductive amination of benzaldehyde and ammonia, which delivered a high catalytic performance for the synthesis of benzylamine from benzaldehyde and ammonia. In the presence of ammonia and H_2, the cation exchange between Co^{2+} and NH_4^+ leads to the formation of $Co(OH)_2$ on $CoBO_x$, which was subsequently reduced to Co nanoparticles. The *in situ* generated Co nanoparticles could suppress the side reactions and realize the selective reductive amination to give primary amine. The selectivity of benzylamine was 95.2% catalyzed by the reconstructed $CoBO_x$, which was obvious higher than Raney Ni, Pt/C or Pt/SiO_2 catalysts. Such an *in situ* reconstruction strategy provided a new approach for the synthesis of the highly performed metallic Co for production of primary amines.

Data availability statement

The original contributions presented in the study are included in the article/Supplementary Material, further inquiries can be directed to the corresponding authors.

Author contributions

MZ designed and conducted the experiments, and wrote the original draft. SZ conducted investigations and edited the manuscript. YM conceptualized the work and edited the manuscript.

Funding

This work was supported by the Fundamental Research Funds for the Central Universities (D5000210283, D5000210601, and D5000210829) and National Natural Science Foundation of China (21872109 and 22002115). SZ was also supported by the Young Elite Scientists Sponsorship Program by CAST (2019QNRC001) and the support of the National Natural Science Foundation of China (Grant No: 22038011).

Conflict of interest

The authors declare that the research was conducted in the absence of any commercial or financial relationships that could be construed as a potential conflict of interest.

Publisher's note

Supplementary material

The Supplementary Material for this article can be found online at: https://www.frontiersin.org/articles/10.3389/fchem.2022.1104844/full#supplementary-material

References

Afanasyev, O. I., Kuchuk, E., Usanov, D. L., and Chusov, D. (2020). Reductive amination in the synthesis of pharmaceuticals. *Chem. Rev.* 119, 11857–11911. doi:10.1021/acs.chemrev.9b00383

Ball, M. R., Wesley, T. S., Rivera-dones, K. R., Huber, G. W., and Dumesic, J. A. (2018). Amination of 1-hexanol on bimetallic $AuPd/TiO_2$ catalysts. *Green Chem.* 20, 4695–4709. doi:10.1039/C8GC02321B

Cabrero-Antonino, J. R., Adam, R., and Beller, M. (2019). Reductive N-alkylations using CO_2 and carboxylic acid derivatives: Recent progress and developments. *Angew. Chem. Int. Ed.* 58, 12820–12838. doi:10.1002/anie.201810121

Chandra, D., Inoue, Y., Sasase, M., Kitano, M., Bhaumik, A., Kamata, K., et al. (2018). A high performance catalyst of shape-specific ruthenium nanoparticles for production of primary amines by reductive amination of carbonyl compounds. *Chem. Sci.* 9, 5949–5956. doi:10.1039/C8SC01197D

Chatterjee, M., Ishizaka, T., and Kawanami, H. (2016). Reductive amination of furfural to furfurylamine using aqueous ammonia solution and molecular hydrogen: An environmentally friendly approach. *Green Chem.* 18, 487–496. doi:10.1039/C5GC01352F

Chen, F., Topf, C. Radnik J., Kreyenschulte, C., Lund, H., Schneider, M., Surkus, A. -E., et al. (2016a). Stable and inert cobalt catalysts for highly selective and practical hydrogenation of C≡N and C═O bonds. *J. Am. Chem. Soc.* 138, 8781–8788. doi:10.1021/jacs.6b03439

Chen, P., Xu, K., Zhou, T., Tong, Y., Wu, J., Cheng, H., et al. (2016b). Strong-coupled cobalt borate nanosheets/graphene hybrid as electrocatalyst for water oxidation under both alkaline and neutral conditions. *Angew. Chem. Int. Ed.* 55, 2488–2492. doi:10.1002/anie.201511032

Dong, B., Guo, X. C., Zhang, B., Chen, X., Guan, J., Qi, Y., et al. (2015). Heterogeneous Ru-based catalysts for one-pot synthesis of primary amines from aldehydes and ammonia. *Catalysts* 5, 2258–2270. doi:10.3390/catal5042258

Dong, C., Wang, H., Du, H., Peng, J., Cai, Y., Guo, S., et al. (2020). Ru/HZSM-5 as an efficient and recyclable catalyst for reductive amination of furfural to furfurylamine. *Mol. Catal.* 482, 110755. doi:10.1016/j.mcat.2019.110755

Gallardo-Donaire, J., Hermsen, M., Wysocki, J., Ernst, M., Rominger, F., Trapp, O., et al. (2018). Direct asymmetric ruthenium-catalyzed reductive amination of alkyl–aryl ketones with ammonia and hydrogen. *J. Am. Chem. Soc.* 140, 355–361. doi:10.1021/jacs.7b10496

Garduño, J. A., and García, J. J. (2020). Toward amines, imines, and imidazoles: A viewpoint on the 3d transition-metal-catalyzed homogeneous hydrogenation of nitriles. *ACS Catal* 10, 8012–8022. doi:10.1021/acscatal.0c02283

Guo, W., Tong, T., Liu, X., Guo, Y., and Wang, Y. (2019). Morphology-tuned activity of Ru/Nb_2O_5 catalysts for ketone reductive amination. *ChemCatChem* 11, 4130–4138. doi:10.1002/cctc.201900335

Irrgang, T., and Kempe, R. (2020). Transition-metal-catalyzed reductive amination employing hydrogen. *Chem. Rev.* 120, 9583–9674. doi:10.1021/acs.chemrev.0c00248

Jagadeesh, R. V., Murugesan, K., Alshammari, A. S., Neumann, H., Pohl, M.-M., Jörg Radnik, J., et al. (2017). MOF-derived cobalt nanoparticles catalyze a general synthesis of amines. *Science* 358, 326–332. doi:10.1126/science.aan6245

Jv, X., Sun, S., Zhang, Q., Du, M., Wang, L., and Wang, Bo. (2020). Efficient and mild reductive amination of carbonyl compounds catalyzed by dual-function palladium nanoparticles. *ACS Sustain. Chem. Eng.* 8, 1618–1626. doi:10.1021/acssuschemeng.9b06464

Kim, J., Kim, H. J., and Chang, S. (2013). Synthetic uses of ammonia in transition-metal catalysis. *Eur. J. Org. Chem.* 16, 3201–3213. doi:10.1002/ejoc.201300164

Komanoya, T., Kinemura, T., Kita, Y., Kamata, K., and Hara, M. (2017). Electronic effect of ruthenium nanoparticles on efficient reductive amination of carbonyl compounds. *J. Am. Chem. Soc.* 139, 11493–11499. doi:10.1021/jacs.7b04481

Lévay, K., and Hegedűs, L. (2018). Selective heterogeneous catalytic hydrogenation of nitriles to primary amines. *Period. Polytech. Chem. Eng.* 62, 476–488. doi:10.3311/PPch.12787

Liang, G., Wang, A., Li, L., Xu, G., Yan, N., and Zhang, T. (2017). Production of primary amines by reductive amination of biomass-derived aldehydes/ketones. *Angew. Chem. Int. Ed.* 56, 3050–3054. doi:10.1002/anie.201610964

Liu, J., Guo, W., Sun, H., Li, R., Feng, Z., Zhou, X., et al. (2019). Reductive amination of carbonyl compounds with ammonia and hydrogenation of nitriles to primary amines with heterogeneous cobalt catalysts. *Chem. Res. Chin. Univ.* 35, 457–462. doi:10.1007/s40242-019-8390-4

Ma, Z., Zhou, B., Li, X., Kadam, R. G., Gawande, M. B., Petr, M., et al. (2022). Reusable Co-nanoparticles for general and selective *N*-alkylation of amines and ammonia with alcohols. *Chem. Sci.* 13, 111–117. doi:10.1039/d1sc05913k

Miller, D. C., Ganley, J. M., Musacchio, A. J., Sherwood, T. C., Ewing, W. R., and Knowles, R. R. (2019). Anti-markovnikov hydroamination of unactivated alkenes with primary alkyl amines. *J. Am. Chem. Soc.* 141, 16590–16594. doi:10.1021/jacs.9b08746

Murugesan, K., Beller, M., and Jagadeesh, R. V. (2019). Reusable nickel nanoparticles-catalyzed reductive amination for selective synthesis of primary amines. *Angew. Chem. Int. Ed.* 58, 5064–5068. doi:10.1002/anie.201812100

Murugesan, K., Senthamarai, T., Chandrashekhar, V. G., Natte, K., Kamer, P. C. J., Beller, M., et al. (2020). Catalytic reductive aminations using molecular hydrogen for synthesis of different kinds of amines. *Chem. Soc. Rev.* 49, 6273–6328. doi:10.1039/C9CS00286C

Nakamura, Y., Kon, K., Touchy, A. S., Shimizu, K., and Ueda, W. (2015). Selective synthesis of primary amines by reductive amination of ketones with ammonia over supported Pt catalysts. *ChemCatChem* 7, 921–924. doi:10.1002/cctc.201402996

Qi, H., Yang, J., Liu, F., Zhang, L., Yang, J., Liu, X., et al. (2021). Highly selective and robust single-atom catalyst Ru_1/NC for reductive amination of aldehydes/ketones. *Nat. Commun.* 12, 3295. doi:10.1038/s41467-021-23429-w

Schranck, J., and Tlili, A. (2018). Transition-metal-catalyzed monoarylation of ammonia. *ACS Catal.* 8, 405–418. doi:10.1021/acscatal.7b03215

Sengupta, M., Das, S., Islam, S. M., and Bordoloi, A. (2020). Heterogeneously catalysed hydroamination. *ChemCatChem* 13, 1089–1104. doi:10.1002/cctc.202001394

Senthamarai, T., Chandrashekhar, V. G., Gawande, M. B., Kalevaru, N. V., Zboril, R., Kamer, P. C. J., et al. (2020). Ultra-small cobalt nanoparticles from molecularly-defined Co-salen complexes for catalytic synthesis of amines. *Chem. Sci.* 11, 2973–2981. doi:10.1039/c9sc04963k

Sukhorukov, A. Y. (2020). Catalytic reductive amination of aldehydes and ketones with nitro compounds: New light on an old reaction. *Front. Chem.* 8, 215. doi:10.3389/fchem.2020.00215

Wang, H., Zheng, Y., Xu, H., Zou, J., Jin, C., J, A., et al. (2022). Metal-free synthesis of N-heterocycles via intramolecular electrochemical C-H aminationsToward amines, imines, and imidazoles: A viewpoint on the 3d transition-metal-catalyzed homogeneous hydrogenation of nitriles. *Front. Chem.ACS Catal.* 1010, 9506358012–9506358022. doi:10.3389/fchem.2022.950635arduñ̃o10.1021/acscatal.0c02283

Yuan, Z., Liu, B., Zhou, P., Zhang, Z., and Chi, Q. (2019). Preparation of nitrogen-doped carbon supported cobalt catalysts and its application in the reductive amination. *J. Catal.* 370, 347–356. doi:10.1016/j.jcat.2019.01.004

Zhang, M., Zou, Y., Zhang, S., and Qu, Y. (2022). *In situ* re-construction of pt nanoparticles interface for highly selective synthesis of primary amines. *ChemCatChem* 14, e202200176. doi:10.1002/cctc.202200176